Proceedings of the 9th World Congress on Momentum, Heat and Mass Transfer (MHMT 2024)
London, United Kingdom – April 11 – 13, 2024
Paper No. ICMFHT 119
DOI: 10.11159/icmfht24.119

Multiphase VOF Modelling of Finite and Infinite Flashing Flow in MSF Desalination

Tarek H Nigim
Mechanical Engineering, University of Galway
Galway, Ireland
nigim@ualberta.ca

Abstract **-** This study investigates the flashing process inside a flashing chamber, which is a key process for desalination in multistage flash (MSF) systems. A new classification of the flashing process as ideal, infinite and finite is proposed. A computational model using a two-phase VOF formulation is developed to simulate the phase-change regions, level and shape of the free surface, and thermofluid behaviour. The model is validated using data from an existing flashing chamber and applied to investigate the effects of finite and infinite flashing processes on flow patterns, and thermal performance. The results suggest that the thermo-fluid behaviour inside the evaporation zone depends on the type of flashing process, either finite or infinite. The study provides insight into the complex, multiphase process of flashing, which is essential for the optimization of MSF desalination systems.

Keywords**:** multiphase; VOF; flashing; thermofluid behaviour; MSF desalination

1. Introduction

The multistage flash (MSF) desalination process is a complex system, and one of its key elements is the flashing chamber, where various phases and fluids interact [1]. In this chamber, energy and mass exchange at its boundaries are essential aspects of its operation, along with the consideration of non-equilibrium temperature difference ($NETD = (T_{outlet} - T_{vapour})$) [2]. Within the flashing chamber, an evaporation zone exists, extending to the brine's free surface, where surface evaporation occurs through a ***self-boiling*** [3] due to a pressure reduction, giving rise to a phase change phenomenon.

The flashing chamber can be divided into distinct layers and regions, as observed by Lior [4]. There are three vertical layers: I, which is the brine flow layer near the base; II, the free surface or brine-vapour interface layer; and III, the vapour layer at the top. Additionally, two horizontal regions are identified: A, comprising the bubble nucleation region near the inlet with a submerged jet and recirculating flow; and B, representing the downstream channel flow, primarily unidirectional.

The flashing process within these chambers can be categorized into three types: ideal, finite, and infinite [5]. The flow field inside the evaporation zone is known for its complexity, being multiphase, turbulent, and unsteady, and featuring various flow patterns and interactions [6].

In this study, we focus on a simplified two-dimensional flow within a flashing chamber without baffles. Understanding the intricacies of this process, including the non-equilibrium temperature difference, is crucial for optimizing the MSF desalination process's efficiency and ensuring sustainable water supplies for communities worldwide. Our primary objective is to employ a multiphase VOF model to predict thermofluid behaviour in the flashing chamber for both finite and infinite flashing flows.

2. CFD Model Description

Our computational model is based on the FLUENT 14.5 two-phase VOF formulation [7, 8] to simulate the flashing process inside a flashing chamber in MSF desalination. The model incorporates two phase-change mechanisms to compute phase-change regions and free surface shape, and is applied to solve for steady multiphase flow inside a flashing chamber without a baffle. The model is limited to a steady-state, two-dimensional model due to the high computational cost and the challenge of assimilating and presenting results from a transient analysis. The simulation results of the model are compared with available measured values, and two main mechanisms of phase change produced by the flashing process are captured. Vapour bubbles are formed at the entrance of the chamber, and bubble production reduces along the length of the chamber. At the free surface of the liquid, there is also a phase change and mass transfer.

2.1. Volume of Fluid (VOF) Multiphase Model

To simulate two-fluid flow dynamics accurately, it is essential to consider factors such as density ratios, temperature jumps across the interface, surface tension effects, topological connectivity, and boundary conditions. Applications involving air-water dynamics, breaking surface waves, solidification melt dynamics, and combustion and reacting flows typically require a two-fluid flow simulation method.

The VOF method, available in the multiphase options of the FLUENT software, is a well-established and validated [9 - 15] approach for tracking interfaces between two or more immiscible fluids in free surface flows. The technique utilizes a group of rectangular cells near the interface to assign appropriate properties and variables to each control volume within the domain based on the local value of the liquid and vapour phase fractions.

The VOF model [7, 8] uses a single set of momentum, energy, and turbulent transport equations for all fluids and computes the volume fraction of each fluid in each computational cell throughout the domain to identify any emerging interfaces. However, it provides information only about the shared properties of the single-fluid mixture, which is its main limitation compared to an Eulerian model that solves individual momentum and continuity equations for each phase.

Fig. 1 depicts a cluster of rectangular cells neighbouring an interface, with the liquid region shown in shaded form. In a flashing simulation, the liquid phase fraction is symbolized by α_l, while the vapour phase is represented by α_v in each cell within the computational domain. Three categories of cells can be identified: empty cells (where α_v), cells that are filled with vapour phase (α_v = 1), and cells that contain the interface between vapour and liquid phase (0 < $\alpha_v \leq 1$). Suitable properties and variables will be assigned to each control volume within the domain, based on the local value of α_v and α_l.

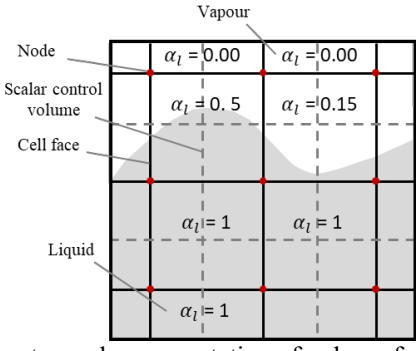

Fig. 1: Discrete mesh representation of volume fraction [16].

2.2. Phase Change Models

Both local thermal effects (saturation temperature) and mechanical effects (vapour pressure) are taken into account in our computational model for predicting flashing flow. Bubble formation and collapse are simulated using an indicator condition based on these mechanisms.

The Lee Wen Ho [17] model is used as a mechanistic model for phase change, representing the transition from liquid to vapour phase and vice versa. Vapourisation-condensation is determined by checking the temperature of the liquid phase (T_l). Mass transfer of the molecules occurs at the liquid-vapour interface, and kinetic energy is a function of the saturation temperature (T_{sat}) of the liquid. The local saturation temperature corresponding to the local pressure of the system is considered as an indicator.

If $T_l > T_{sat}$ (vapourisation), then

$$\dot{m}_{l\to v} = (coeff)\ \alpha_l \rho_l \frac{(T_l - T_{sat})}{T_{sat}} \tag{1}$$

If $T_v \leq T_{sat}$ (condensation), then

$$\dot{m}_{v\to l} = (coeff)\ \alpha_v \rho_v \frac{(T_v - T_{sat})}{T_{sat}} \tag{2}$$

where, $\dot{m}_{l\to v}$ = mass transfer rate from liquid to vapour phase, $\dot{m}_{v\to l}$ = mass transfer rate from vapour phase to liquid. liquid. α_v=vapour phase fraction, ρ_v=density of vapour [kg/m^3], ρ_l= density of liquid [kg/m^3].

The coefficient, , needs to be adjusted carefully to obtain the most accurate representation of performance. It is also referred to as a relaxation. To facilitate preliminary calculations when the diameter of the vapour bubbles is unknown, we set the value of $coeff$ to 0.1, eliminating the need to define the diameter.

The mechanical effect is captured by an indicator based on a model proposed by Zwart et al. [18] and derived from the generalized Rayleigh-Plesset equation. The indicator assumes that all bubbles in the system are of the same size, and vapour bubbles nucleate and grow when the local pressure of the phase is lower than the local saturation pressure. Conversely, vapour bubbles collapse and disappear when the local pressure (p) of the phase is greater than the local saturation pressure (p_v). The indicator condition is developed based on these principles.

If $p \leq p_v$, then

$$R_e = F_{vap} \frac{3\ \alpha_{nuc}(1 - \alpha_v)\rho_v}{R_b} \sqrt{\frac{2}{3}\frac{P_v - P}{\rho_l}} \tag{3}$$

If $p \geq p_v$, then

$$R_c = F_{col} \frac{3\alpha_v\ \rho_v}{R_b} \sqrt{\frac{2}{3}\frac{P - P_v}{\rho_l}} \tag{4}$$

where, R_e= mass transfer source term connected to the growth of the vapour bubbles, R_c = mass transfer source term connected to the collapse of the vapour bubbles. , F_{vap}= vaporization coefficient = 50, α_{nuc} = nucleation site volume fraction = 5*10^{-4}, R_b = bubble radius = 10^{-6} m, F_{col} = collapse coefficient = 0.01.

3. Computational Case Setup and Validation

In our present work, the computational model is developed to simulate the evaporation zone in the first flashing chamber of a multi-stage flash (MSF) desalination plant, and its validity is assessed against data obtained from the Sidi Krir plant in Alexandria, Egypt. The computational domain's size (Fig. 2) and operating conditions are obtained from published literature [19, 20]. The domain consists of the chamber's geometry, which is bounded by walls on three sides, with one inlet and one outlet for the brine. The mesh generation involves 201,358 elements with six inflation layers near the walls as shown in (Fig. 2). Mesh refinement extends into the viscous sublayer near solid surfaces to improve accuracy [7] in resolving near-wall flows. Wall functions and k-ε turbulence model are utilized. The model is based on a 2D, steady-state, adiabatic, turbulent, and two-phase flow of liquid water and water vapour, with no consideration for surface roughness. The pressure-based solution algorithm is used to derive the pressure, and the PISO algorithm is employed to resolve the pressure-velocity coupling. The study uses a collocated scheme in which all variables, including velocity and pressure, are stored at cell centers. To enhance precision, the convective terms in the momentum, volume fraction, turbulence variables, and energy equations undergo spatial discretization using second-order upwind differencing. The values of fluid properties are estimated from published sources [21, 22], and the vapour pressure is a function of the local temperature. The simulation's accuracy is determined by comparing the model's results with the measured values obtained from the Sidi Krir plant.

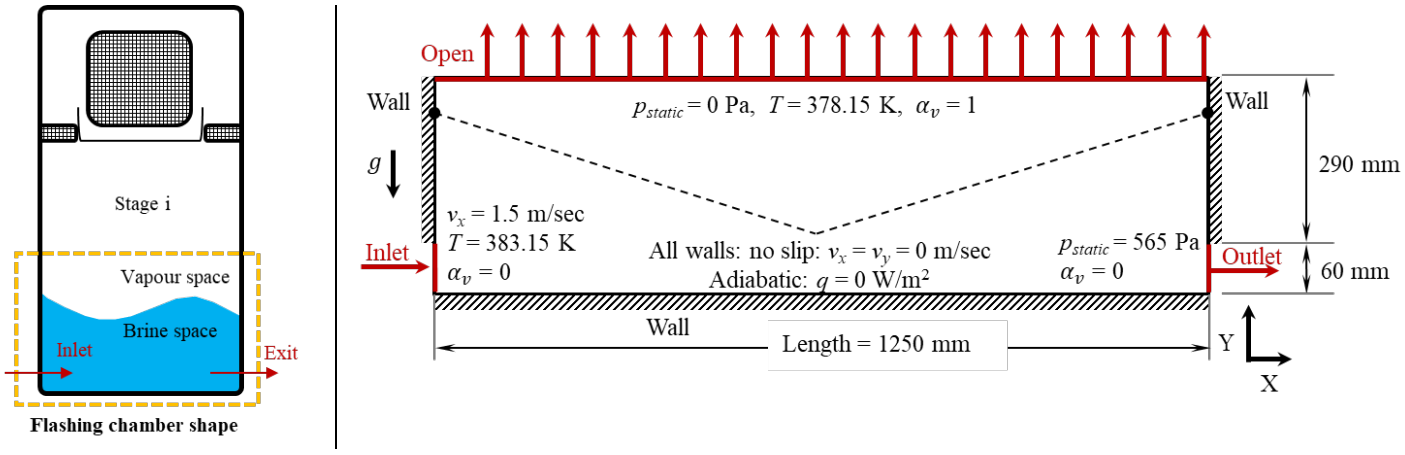

Fig. 2: Flashing chamber dimensions and boundary conditions [19]. Typical computational domain mesh inside the flashing chamber.

3.1. Mesh Resolution

In the analysis of multiphase flow featuring phase change and free surface prediction, accurate results necessitate the meticulous selection of mesh size. It is critical to employ a mesh size that is small, gradual, and lacking sudden changes in cell size to prevent the omission of phase change zones and achieve flow field resolution. The initial application of a coarse mesh aimed to establish mesh independence, as per the recommendation of [19, 20]. A range of meshes with quadrilateral rectangular shape elements, encompassing coarse (1.6 x 1.6 mm), medium (1.4 x 1.4 mm), and fine (1.2 x 1.2 mm) meshes, were subsequently evaluated using the current model and identical boundary and initial conditions as presented in (Fig. 2.) The pertinent variables, temperature, velocity magnitude, and vapour volume fraction, were extracted by traversing the flashing chamber at x = 0.6 m, randomly as shown in (Fig. 3). Comparison of the predicted results showed that the maximum differences were insignificant, with temperature distribution, velocity distribution, and vapour volume fraction distribution being less than 0.03°C, 0.05 m/s, and 0.00625, respectively. These findings suggest mesh independence. To ensure precision, the outlet average temperature was compared for all three mesh sizes. The fine mesh size (378.7 K) exhibited the highest accuracy compared to the given outlet temperature of 379 K [19, 20]. Consequently, the fine mesh size was applied in all subsequent study cases.

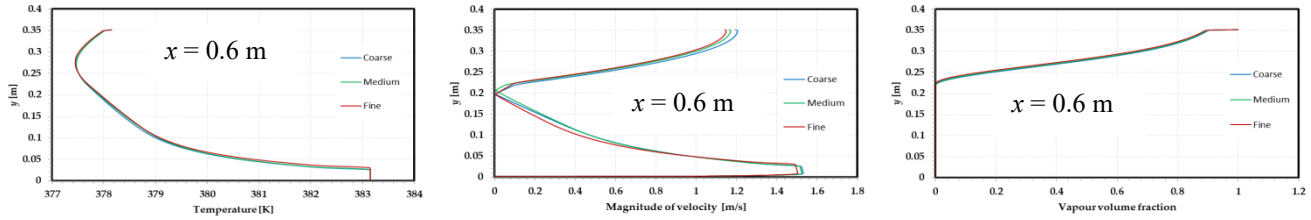

Fig. 3: Influence of mesh size on (a) temperature , (b) mixture speed, (c) vapour volume fraction along a vertical traverse through the flashing chamber at x/L = 0.5.

3.2. Validation

Obtaining sufficient data to build and validate a computational model is the main challenge in predicting the behaviour of the flashing chamber. Specifically, gathering information about the interior of the chamber, such as bubble nucleation rate, bubble formation, recirculation zone size and length, brine level, and orifice shapes and numbers, is difficult. Additionally, the limited available data often lack information about measurement locations, methods, and uncertainties. The VOF multiphase model, established and validated [9 - 15] in predicting liquid-gas

interfaces and free surface shapes in various applications, including the mechanistic Lee Wen Ho [17] vaporization-condensation model, has been used for the prediction of vapour volume fraction. Our implementation of the Zwart et al. al. vaporization-condensation model [18] within the Fluent VOF code was validated [3] using data from extensive experiments for isothermal flashing water flow in a converging-diverging nozzle by Abuaf et al. [23]. Our simulation of of the evaporation zone of the flashing chamber was validated by comparing the average temperature at the stage exit, and average vapour temperature above the liquid free surface, with available data, resulting in good agreement with the values for the real plant presented in (Table 1).

Table 1: Comparison of predicted results and measured values.

	Measured	**Predicted**	**Relative Error[%]**
Average outlet temperature[K]	379	378.6	0.1
Average vapour temperature[K]	375	377.7	0.7

The simulation of the flashing process (Fig. 4) shows consistency with the mechanism illustrated in § Introduction. Fig. 4 indicates that vapour bubbles are formed at the entrance of the flashing chamber, and their generation decreases as they move along its length. Furthermore, the simulation successfully captures the phase change and mass transfer occurring at the free surface of the liquid, which are the two primary mechanisms of phase change resulting from the flashing process. Regarding the brine level, the simulation predicts a level of 0.2m above the inlet, in agreement with the design recommendations proposed by El-Dessouky et al. [24]. These recommendations suggest that the brine pool should be higher than the gate height by 0.2m.

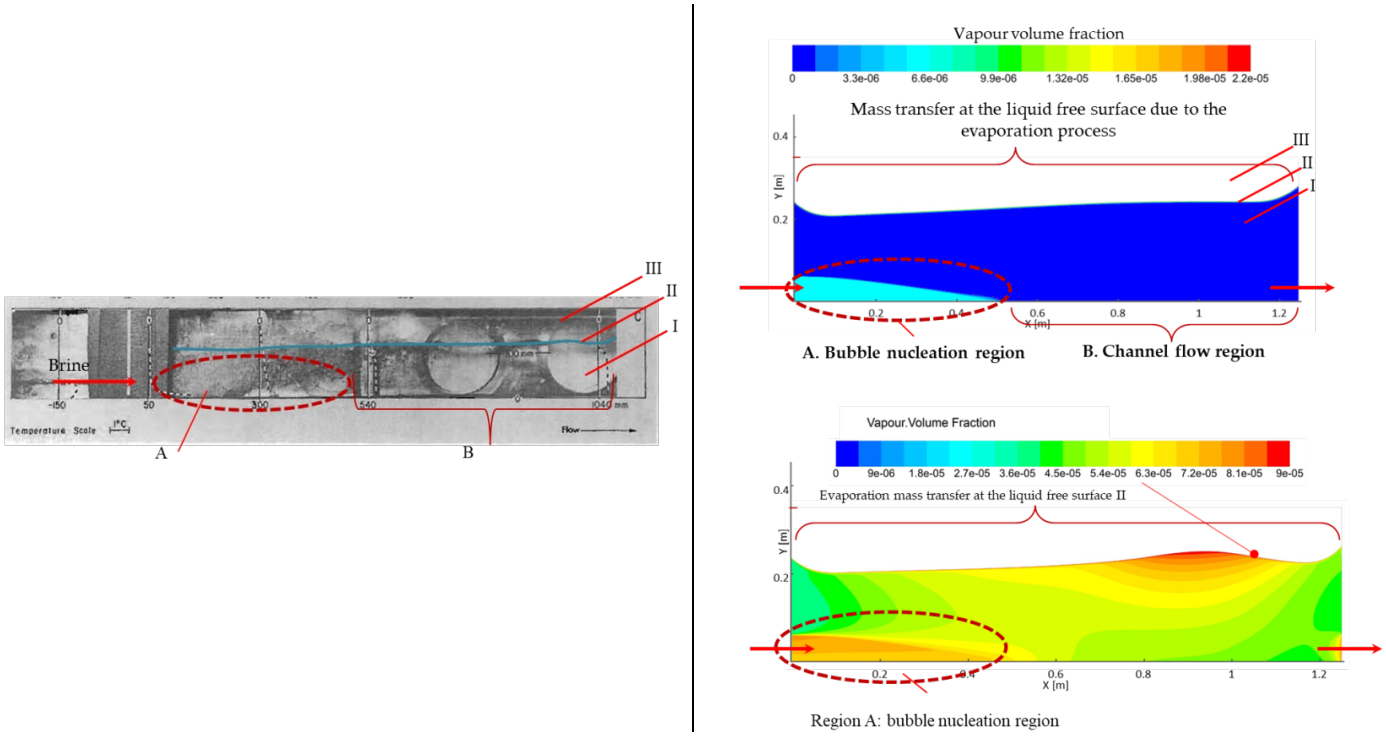

Fig. 4: (a) Flashing regions of the flashing chamber (adapted from Lior, 1980). Flashing regions in the flashing chamber as predicted by computational model under (b) Finite Flashing (c) Infinite Flashing conditions.

4. Results

The developed model demonstrated the ability to accurately predict the free surface level and shape, as well as visualize the flashing process and phase change regions throughout the prediction field, regardless of whether it occurs under finite or infinite flashing flow conditions (Fig. 4).

Fig. 5 shows the flow fields observed in both finite and infinite flashing scenarios. These fields are characterized by the velocity magnitude and vector map with fixed length vectors, which are measured across the flashing chamber. Due to low tangential shear stress, the velocity magnitude near the free surface is significantly low. Additionally, the mixture comprises a higher proportion of vapour than the liquid phase above and away from the free surface, resulting in an increase in fluid speed due to the mixture density effect.

As shown in (Fig. 5), the fluid movement is relatively high in the bubble nucleation region, which subsequently decreases along the channel flow region. However, at the brine exit, the fluid accelerates to the maximum due to area reduction.

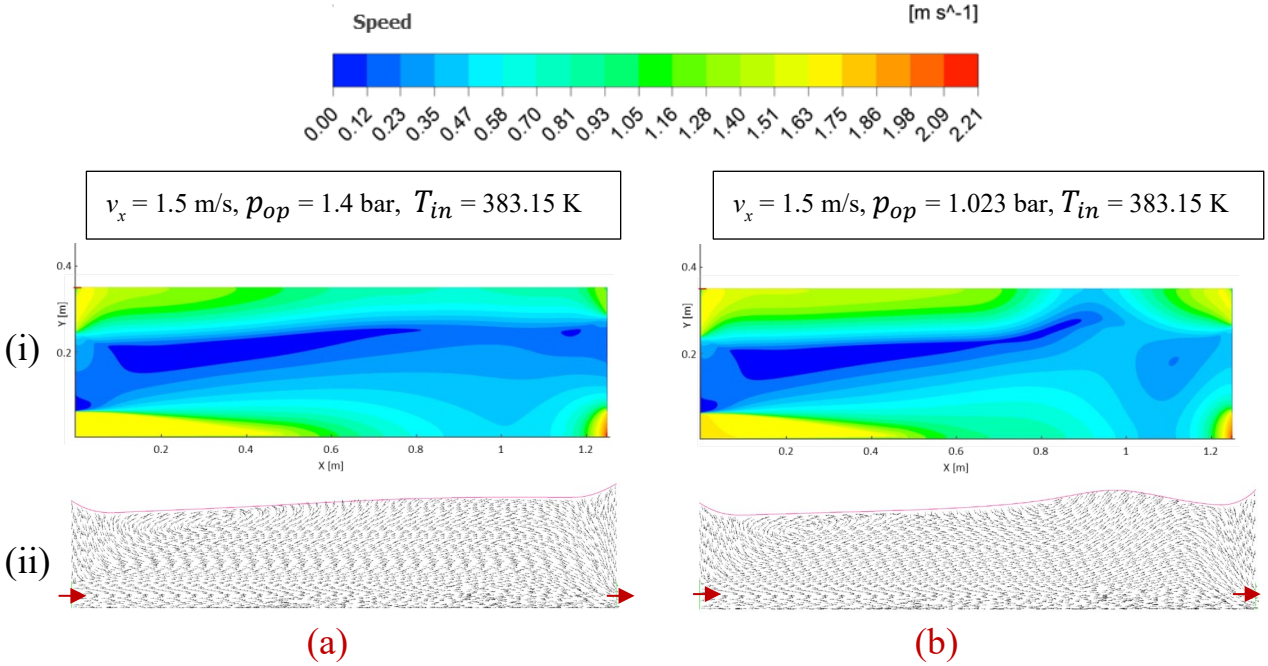

Fig. 5: Predicted flow fields: (i) velocity magnitude, and (ii) vector map with fixed length vectors for (a) finite and (b) infinite flashing flow.

The thermal performance of both finite and infinite flashing flows is shown in (Fig. 6). The rate of flashing is directly linked to the thermal performance, or brine temperature field. The flashing process reduces the brine temperature, as demonstrated by the overall temperature field and the horizontal temperature traverses displayed in (Fig. 6) The temperature decrease occurs in both the horizontal (x-) and vertical (y-) directions, but in different rates.

5. Discussion

This study examines particle paths and velocity distribution in both finite and infinite flashing conditions. In infinite flashing, the minimum velocity at the free surface maintains mass conservation, while a maximum speed of 1.88 m/s at the chamber's end upholds the conservation of energy. In finite flashing, the maximum speed is 1.9 m/s, also confirming energy conservation. The recirculation zone aids in bubble transport to the free surface, shedding light on the relationship between fluid flow and thermal behaviour, including turbulent kinetic energy conversion for vertical heat flow prediction.

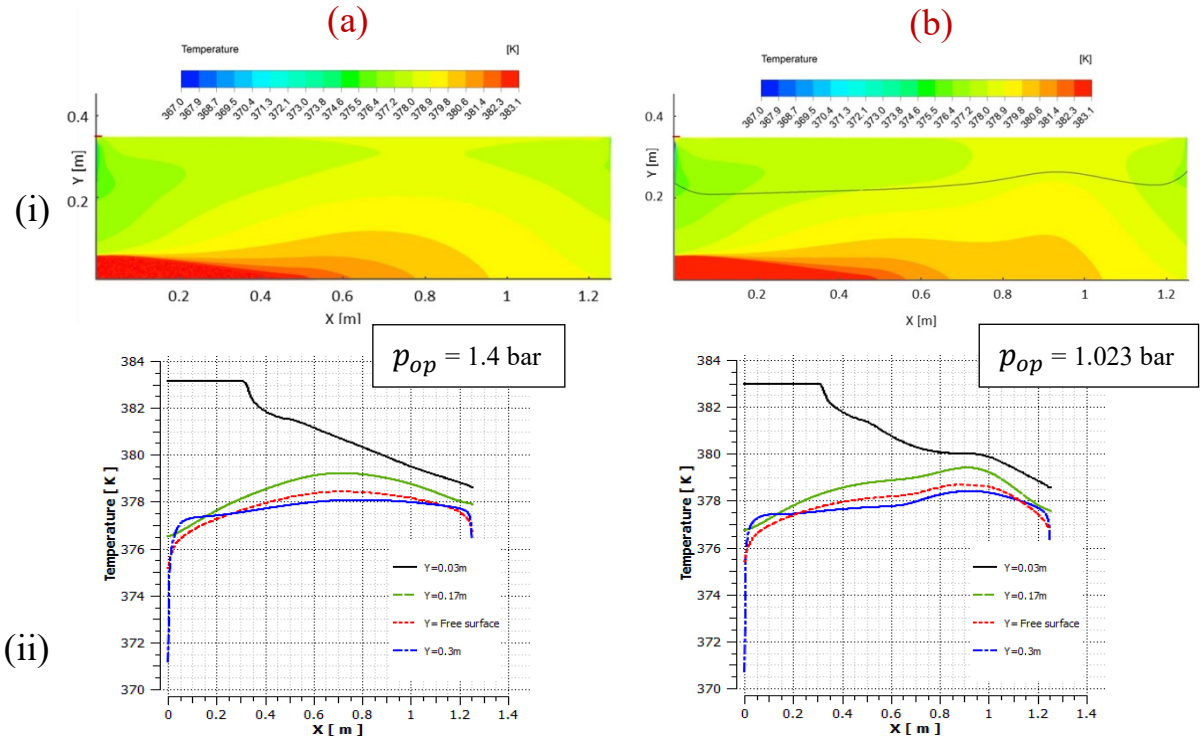

Fig. 6: (i) Predicted temperature field, and (ii) temperature distribution along horizontal traverses at y = 0.03m, 0.17m, free surface line, 0.3m for (a) finite and (b) infinite flashing flow.

The inlet velocity profile is a critical fluid dynamic parameter influencing the flashing process. Careful consideration of the inlet velocity profile is necessary for inter-stages and the final flashing chamber. An analysis showed that a uniform inlet velocity profile results in the closest average outlet temperature compared to available plant data, with tests conducted using three different unidirectional flow cases with varying inlet profiles [25].

The thermal performance of the flashing process varies between finite and infinite conditions. In infinite flashing, the temperature reduction due to phase change influences mass transfer and vapour distribution. Vertical temperature gradients dominate due to turbulent shear mixing, favouring vertical heat transfer. Positive *NETD* is observed as the exit brine temperature exceeds the saturation temperature corresponding to the operating pressure. In finite flashing, the brine temperature decreases until reaching saturation temperature, after which no further phase change occurs. The exit brine temperature is lower than the saturation temperature, resulting in a negative *NETD*. Understanding these differences in thermal performance is crucial for designing and optimizing the flashing process, aiming for higher efficiency and reduced energy consumption.

Within the domain of CFD, we must underscore the significance of subtle result variations. For instance, a mere 0.1% difference in validation outcomes, as observed using the VOF model, can have substantial real-world ramifications. In industries with stringent performance standards, even a one degree temperature change can lead to significant energy losses and reduced system efficiency, underscoring the need for precision in CFD simulations, especially in multiphase contexts.

6. Summary and Conclusion

A numerical method was developed to predict the multiphase flow field during flashing flow using a FLUENT VOF code implementation. The model considered thermal and mechanical effects for phase change during the flashing process and was tested with three different mesh sizes to ensure accuracy. The model was evaluated for MSF desalination systems and found to match real plant values. Infinite and finite flashing were classified, and their effects on the flashing chamber

performance were analysed based on operational parameters. The simulation results provided insights into heat transfer, mass transfer, and fluid dynamics during the flashing flow evaporation process. Design factors such as non-equilibrium temperature difference, flashing down, and flashing efficiency were estimated. The computational method can assist in the design and optimization of MSF systems by identifying ideal operating conditions and system parameters. Overall, this study provides valuable information for the design and optimization of MSF desalination systems through computational modelling.

Acknowledgements

This work was funded through a postgraduate Research Fellowship from the College of Engineering and Informatics, University of Galway, IRELAND.

References

[1] A.H. Khan, "Desalination Processes and Multi-Stage Flash Distillation Practice," Elsevier, Amsterdam, 1986.
[2] R. Rautenbach, S. Schäfer, and S. Schleiden, "Improved equations for the calculation of non-equilibrium temperature loss in MSF," *Desalination*, vol. 108, pp. 325–333, 1996.
[3] T. H. Nigim and J. A. Eaton, "CFD prediction of flashing processes in a MSF desalination chamber," *Desalination*, vol. 420, pp. 258-272, 2017.
[4] N. Lior, "Some basic observations on heat transfer and evaporation in the horizontal flash evaporator," *Desalination*, vol. 33, pp. 269-286, 1980.
[5] T. H. Nigim, "Novel classification of multistage flash desalination via finite and infinite flashing: Investigating thermofluid dynamics under varying inlet flow rates employing validated multiphase CFD simulations," *Computers & Chemical Engineering*, vol. 179, 2023.
[6] O. Miyatake, T. Fujii, T. Tanaka, and T. Nakaoka, "Flash evaporation phenomena of pool water," *Heat Transfer Jpn. Res.*, vol. 1, pp. 393-398, 1975.
[7] ANSYS Fluent Theory Guide, Release 14.5, 2016.
[8] J. H. Ferziger and M. Peric, "Computational Methods for Fluid Dynamics," Springer, New York, 2002.
[9] W.F. Noh and P. Woodward, "SLIC (Simple Line Interface Calculation)," in *Proceedings, Fifth International Conference on Fluid Dynamics*, A.I. van de Vooren and P.J. Zandbergen, Eds., Lecture Notes in Physics 59, Berlin, Springer, 1976, pp. 330-340.
[10] B.D. Nichols and C.W. Hirt, "Numerical simulation of boiling water reactor vent-clearing hydrodynamics," *Nuclear Science and Engineering*, vol. 73, pp. 196-209, 1980.
[11] C.W. Hirt and B.D. Nichols, "Volume of fluid (VOF) method for the dynamics of free boundaries," *Journal of Computational Physics*, vol. 39, pp. 201-225, 1981.
[12] S. Kvicinsky, F. Longatte, J.L. Kueny, and F. Avellan, "Free surface flows: experimental validation of volume of fluid (VOF) method in the plane wall case," in *Proceedings of the 3rd ASME, JSME Joint Fluids Engineering Conference*, San Francisco, California, 1999.
[13] R. Saurel and R.A. Abrall, "Multiphase Godunov method for compressible multifluid and multiphase flows," *Journal of Computational Physics*, vol. 150, pp. 425-467, 1999.
[14] D.M. Hargreaves, H.P. Morvan, and N.G. Wright, "Validation of the volume of fluid method for free surface calculation: the broad-crested weir," *Engineering Applications of Computational Fluid Mechanics*, vol. 1, pp. 136-146, 2007.
[15] V. Hernandez-Perez, "Gas-Liquid Two-Phase Flow in Inclined Pipes," Ph.D. thesis, University of Nottingham, 2008.
[16] T.H. Nigim and J.A. Eaton, "Simulation of the flashing processes in a MSF desalination stage," in *Desalination for the Environment: clean Water and Energy*, EDS, Rome, Italy, May 2016.
[17] W.H. Lee, "A Pressure Iteration Scheme for Two-phase Modeling," Technical Report LA-UR 79-975, Los Alamos Scientific Laboratory, Los Alamos, New Mexico, 1979.
[18] P.J. Zwart, A.G. Gerber, and T.A. Belamri, "Two-phase flow model for predicting cavitation dynamics," in *Fifth International Conference on Multiphase Flow*, Yokohama, Japan, 2004.
[19] K.M. Mansour and H.E.S. Fath, "Numerical simulation of flashing process in MSF flash chamber," *Desalination and Water Treatment*, vol. 51, pp. 2231-2243, 2013.
[20] K.M. Mansour, H.E.S. Fath, and O. El-Samni, "Computational fluid dynamics study of MSF flash chambers sub-components; I – vapor flow through demister," in *The Fifteenth International Water Technology Conference, IWTC15*, Alexandria, Egypt, 2011.
[21] N.B. Vargaftik, B.N. Volkov, and L.D. Voljak, "International tables of the surface tension of water," *Journal of Physical and Chemical Reference Data*, vol. 12, pp. 817-820, 1983.
[22] M.H. Sharqawy, J.H. Lienhard V, and S.M. Zubair, "Thermophysical properties of seawater : a review of existing correlations and data," *Desalination and Water Treatment*, vol. 16, pp. 354-380, 2010.
[23] N. Abuaf, B.J.C. Wu, G.A. Zimmer, and P. Saha, "A Study of Non-Equilibrium Flashing Of Water in a Converging-Diverging Nozzle: Volume 1 – Experimental," United States Nuclear Regulatory Commission Office of Nuclear Regulatory Research, 1981.
[24] H.T. El-Dessouky and H.M. Ettouney, "Fundamentals of Salt Water Desalination," Elsevier Science B.V., Amsterdam, the Netherlands, 2002.
[25] T. H. Nigim, "Computational Modelling of Thermofluid Flashing in MSF Desalination," Ph.D. Dissertation, University Galway, 2017.